



## Chemical reaction and thermal radiation effects on MHD micropolar fluid past a stretching sheet embedded in a non-Darcian porous medium

L. Ramamohan Reddy<sup>a</sup>, M. C. Raju<sup>b\*</sup>, G. S. S. Raju<sup>c</sup> and S. M. Ibrahim<sup>d</sup>

<sup>a</sup>Department of Mathematics, Mekapati Rajamohan Reddy Institute of Technology and Science, Udayagiri, Nellore District, A.P, India

<sup>b</sup>Department of Humanities and Sciences, Annamacharya Institute of Technology and Sciences (Autonomous), Rajampet – 516126, A.P., India

<sup>c</sup>Department of Mathematics, JNTUA College of Engineering Pulivendula, Pulivendula, A.P, India

<sup>d</sup>Department of Mathematics, GITAM University, Vishakhapatnam, A.P. - 530045 India

---

### Article info:

Received: 12/02/2016

Accepted: 17/04/2016

Online: 03/03/2017

---

### Keywords:

MHD,  
Micropolar fluid,  
Chemical reaction,  
Thermal radiation,  
VUMAT subroutine,  
Porous medium.

### Abstract

The paper aims at investigating the effects of chemical reaction and thermal radiation on the steady two-dimensional laminar flow of viscous incompressible electrically conducting micropolar fluid past a stretching surface embedded in a non-Darcian porous medium. The radiative heat flux is assumed to follow Rosseland approximation. The governing equations of momentum, angular momentum, energy, and species equations are solved numerically using Runge-Kutta fourth order method with the shooting technique. The effects of various parameters on the velocity, microrotation, temperature and concentration field as well as skin friction coefficient, Nusselt number and Sherwood number are shown graphically and tabulated. It is observed that the micropolar fluid helps the reduction of drag forces and also acts as a cooling agent. It was found that the skin-friction coefficient, heat transfer rate, and mass transfer rate are decreased, and the gradient of angular velocity increases as the inverse Darcy number, porous medium inertia coefficient, or magnetic field parameter increase. Increases in the heat generation/absorption coefficient caused increases in the skin-friction coefficient and decrease the heat transfer rate. It was noticed that the increase in radiation parameter or Prandtl number caused a decrease in the skin-friction coefficient and an increase in the heat transfer rate. In addition, it was found that the increase in Schmidt number and chemical reaction caused a decrease in the skin-friction coefficient and an increase in the mass transfer rate.

### 1. Introduction

In recent years, the dynamics of micropolar fluids, originating from the theory of Eringen

[1], has been a popular area of research. This theory takes into account the effect of local rotary inertia and couple stresses arising from practical microrotation action. This theory is

---

\*Corresponding author

email address: [mcrmaths@yahoo.co.in](mailto:mcrmaths@yahoo.co.in)

applied to suspensions, liquid crystals, polymeric fluids, and turbulence. This behavior is familiar in many engineering and physical applications. Also, the study of boundary layer flows of micropolar fluids over a stretching surface has received much attention because of their extensive applications in the field of metallurgy and chemical engineering for example, in the extrusion of polymer sheet from a die or in the drawing of plastic films. Na and Pop [2] investigated the boundary layer flow of a micropolar fluid past a stretching wall. Desseaux and Kelson [3] studied the flow of a micropolar fluid bounded by a stretching sheet. Hady [4] studied the solution of heat transfer to micropolar fluid from a non-isothermal stretching sheet with injection. However, recently, the effects of a magnetic field on the micropolar fluid problem are very important.

The problem of stretching sheet under the influence of magnetic field is also an interesting problem of research. Such investigations of magneto hydrodynamics (MHD) flows are industrially important and have applications in different areas of research such as petroleum production, geophysical flows, cooling of underground electric cables, etc. It has been found that the application of a magnetic field reduces the heat transfer at the stagnation point and increases the skin friction. These features are useful in the design of heat shield for protecting the spacecraft entering or re-entering the atmosphere. Aydin et al. [5] analyzed Non-Darcian forced convection flow of a viscous dissipating fluid over a flat plate embedded in a porous medium. Das et al. [6] presented mass transfer effects on MHD flow and heat transfer past a vertical porous plate through a porous medium under oscillatory suction and heat source.

Non-Darcy behavior is important for describing fluid flow in porous media in situations where high velocity occurs. A criterion to identify the beginning of non-Darcy flow is needed. Two types of criteria, the Reynolds number, and the Forchheimer number have been used in the past for identifying the beginning of non-Darcy flow. Many transport processes exist in nature and in industrial applications in which the simultaneous heat and mass transfer occur as a result of

combined buoyancy effects of thermal diffusion and diffusion of chemical species. A few representative fields of interest in which combined heat and mass transfer plays an important role are designing of chemical processing equipment, formation and dispersion of fog, distribution of temperature and moisture over agricultural fields and groves of fruit trees, crop damage due to freezing, and environmental pollution. Ananda Rao et al. [7] obtained chemical reaction effects on an unsteady MHD free convective flow past an infinite vertical porous plate with constant suction and heat source. Ibrahim et al. [8] discussed radiation effect on chemically reacting MHD boundary layer flow of heat and mass transfer through a porous vertical flat plate. Pal et al. [9] investigated combined effects of Joule heating and chemical reaction on an unsteady magneto hydrodynamic mixed convection of a viscous dissipating fluid over a vertical plate in porous media with thermal radiation. Jhansi Rani et al. [10] studied MHD flow over a moving infinite vertical porous plate with uniform heat flux in the presence of thermal radiation. Reddy et al. [11] assumed heat and mass transfer effects on MHD free convection flow past an oscillating plate embedded in a porous medium. Reddy et al. [12] considered an unsteady MHD radiative and chemically reactive free convection flow near a moving vertical plate in a porous medium. Raju et al. [13] studied the MHD thermal diffusion natural convection flow between heated inclined plates in a porous medium. Chandrakala et al. [14] solved radiation effects on flow past an impulsively started vertical oscillating plate with a uniform heat flux. Choudhury et al. [15] established MHD mixed convective heat and mass transfer in a viscoelastic boundary layer slip flow past a vertical permeable plate with thermal radiation and chemical reaction. Abzal et al. [16] examined MHD free convection flow and unsteady mass transfer near a moving vertical plate in the presence of thermal radiation. Ravikumar et al. [17] investigated magnetic field and radiation effects on a double diffusive free convective flow bounded by two infinite impermeable plates in the presence of chemical reaction. Mohamed et al. [18] obtained an

unsteady MHD double diffusive convection boundary-layer flow past a radiate hot vertical surface in porous media in the presence of chemical reaction and heat sink. Malik et al [19] studied MHD flow of a tangent hyperbolic fluid over a stretching cylinder using Keller box method. The effect of a transverse magnetic field with a variable thermal conductivity on a tangent hyperbolic fluid with an exponentially varying viscosity was investigated by Salahuddin et al. [20]. Salahuddin et al. [21] proposed MHD flow of cattaneo-Christov heat flux model for Williamson fluid over a stretching sheet with a variable thickness.

Seshaiah et al. [22] presented the effects of chemical reaction and radiation on unsteady MHD free convective fluid flow embedded in a porous medium with time-dependent suction with temperature gradient heat source. Rout et al. [23] analyzed chemical reaction and radiation effects on MHD flow past an exponentially accelerated vertical plate in presence of heat source with variable temperature embedded in a porous medium. Khan et al. [24] discussed the Cheng-Minkowycz problem of the triple-diffusive natural convection boundary layer flow past a vertical plate in a porous medium. Seth et al. [25] investigated effects of thermal radiation and rotation on unsteady hydro magnetic free convection flow past an impulsively moving vertical plate with ramped temperature in a porous medium. Kesavaiah et al. [26] studied effects of the chemical reaction and radiation absorption on an unsteady MHD convective heat and mass transfer flow past a semi-infinite vertical permeable moving plate embedded in a porous medium with heat source and suction. Rajput et al. [27] studied radiation effects on MHD flow past an impulsively started vertical plate with variable heat and mass transfer. Muthukumaraswamy et al. [28] noticed the influence of the variable mass diffusion on convective flow past an accelerated isothermal vertical plate in rotating fluid in presence of chemical reaction. Devika et al. [29] considered MHD oscillatory flow of a visco elastic fluid in a porous channel with chemical reaction. Chand et al. [30] established Hall effect on radiating and chemically reacting MHD oscillatory flow in a rotating porous vertical channel in a slip flow

regime. Mukhopadhyay et al. [31] examined effects of partial slip on boundary layer flow past a permeable exponential stretching sheet in the presence of thermal radiation. Kameswaram et al. [32] obtained homogeneous-heterogeneous reactions in a nanofluid flow due to a porous stretching sheet. Shaw et al. [33] presented homogeneous-heterogeneous reactions in a micropolar fluid flow from a permeable stretching or shrinking sheet in a porous medium. Ellahi et al. [34] analyzed non-Newtonian nanofluid flow through a porous medium between two coaxial cylinders with heat transfer and variable viscosity. Bachok et al. [35] discussed boundary layer stagnation-point flow and heat transfer over an exponentially stretching/ shrinking sheet in a nanofluid. Akbar et al. [36] investigated radiation effects on MHD stagnation point flow of a nanofluid towards a stretching surface with convective boundary condition. Sheikholeslami et al. [37] studied effect of thermal radiation on MHD nanofluid flow and heat transfer by means of two phase models. Turkyilmazoglu et al. [38] assumed heat and mass transfer of an unsteady natural convection flow of some nanofluids past a vertical infinite flat plate with radiation effect. Sheikholeslami et al. [39] considered ferrofluid flow and heat transfer of a semi annulus enclosure in the presence of magnetic source considering thermal radiation. Pal [40] studied combined effects of non-uniform heat source/sink and thermal radiation on heat transfer over an unsteady stretching permeable surface. Shit et al. [41] solved effects of thermal radiation on MHD viscous fluid flow and heat transfer over a nonlinear shrinking porous sheet. Das [42] examined impact of thermal radiation on MHD slip flow over a flat plate with variable fluid properties. Akyildiz et al. [43] studied existence results of third order nonlinear boundary value problems arising in nano boundary layer fluid flows over stretching surfaces. Chamkha et al. [44] presented et al non-similar solution for natural convective boundary layer flow over a sphere embedded in a porous medium saturated with a nanofluid. Bachok et al. [45] analyzed stagnation-point flow over a stretching/shrinking sheet in a nanofluid. Makinde et al. [46] studied boundary layer flow

of a nanofluid past a stretching sheet with a convective boundary condition.

Motivated by the previous works and possible applications, this paper studies the interaction of radiation and chemical reaction of an electrically conducting micropolar fluid past a stretching surface which has received little attention. Hence an attempt is made to investigate the radiation effects on a steady free convection flow near an isothermal vertical stretching sheet in the presence of a magnetic field, a non-Darcian porous medium and chemical reaction. The governing equations are transformed by using similarity transformation, and the resultant dimensionless equations are solved numerically using the Runge-Kutta fourth order method with the shooting technique. The effects of various governing parameters on the velocity, temperature, concentration, skin-friction coefficient, the Nusselt number, and Sherwood number are shown in the figures and tables and analyzed in detail.

## 2. Mathematical formulation

Let us consider a steady, two-dimensional laminar, free convection boundary layer flow of an electrically conducting dissipative and heat generating micropolar fluid through a porous medium bounded by a vertical isothermal stretching sheet coinciding with the plane  $y = 0$ , where the flow confined to  $y > 0$ . Two equal and opposite forces are introduced along the  $x'$  - axis so that the sheet is linearly stretched keeping the origin fixed. A uniformly distributed transverse magnetic field of strength  $B_0$  is imposed along the  $y'$  - axis. The magnetic Reynolds number of the flow is taken to be small enough so that the induced distortion of the applied magnetic field can be neglected. It is also assumed that microscopic inertia term involving  $J$  (where  $J$  is the square of the characteristic length of microstructure) can be neglected for steady two-dimensional boundary layer flow in a micropolar fluid without introducing any appreciable error in the solution. Under the above assumptions and upon treating the fluid saturated porous medium as continuum, including the non-Darcian inertia effects, and assuming that the Boussinesq

approximation is valid, the boundary layer form of the governing equations can be written as.

Continuity equation

$$\frac{\partial u'}{\partial x'} + \frac{\partial v'}{\partial y'} = 0 \tag{1}$$

Momentum equation

$$u' \frac{\partial u'}{\partial x'} + v' \frac{\partial u'}{\partial y'} = \nu \frac{\partial^2 u'}{\partial y'^2} + g\beta(T' - T'_\infty) \tag{2}$$

$$+ g\beta^*(C' - C'_\infty) + k_1 \frac{\partial \sigma'}{\partial y'} - \frac{\sigma_0 B_0^2}{\rho} u' - \frac{\nu}{K} u' - C_1 u'^2$$

Angular Momentum equation

$$G_1 \frac{\partial^2 \sigma'}{\partial y'^2} - 2\sigma' - \frac{\partial u'}{\partial y'} = 0 \tag{3}$$

Energy equation

$$u' \frac{\partial T'}{\partial x'} + v' \frac{\partial T'}{\partial y'} = \frac{k_e}{\rho c_p} \frac{\partial^2 T'}{\partial y'^2} - \frac{1}{\rho c_p} \frac{\partial q_r}{\partial y'} \tag{4}$$

species equation

$$u' \frac{\partial C'}{\partial x'} + v' \frac{\partial C'}{\partial y'} = D \frac{\partial^2 C'}{\partial y'^2} - K'_r (C' - C'_\infty) \tag{5}$$

subject to the boundary conditions

$$u' = bx, v' = 0, T' = T'_w, C' = C'_w, \sigma = 0 \text{ at } y = 0, \\ u' \rightarrow u'_\infty, T' \rightarrow T'_\infty, C' \rightarrow C'_\infty, \sigma = 0 \text{ as } y \rightarrow \infty \tag{6}$$

where  $x'$  and  $y'$  are the coordinates along and normal to the sheet.  $u'$  and  $v'$  are the components of the velocity in the  $x'$  and  $y'$  - directions, respectively.  $\sigma, k_1$  and  $G_1$  are the micro-rotation component, coupling constant, and micro-rotation constant, respectively.  $k_e, C_1, K$  are the effective thermal conductivity, permeability of the porous medium, transport property related to the inertia effect.  $T'$  is fluid temperature,  $C'$  is fluid concentration.  $T'_w$  is the surface temperature,  $C'_w$  is the surface concentration,  $T'_\infty$  be the ambient temperature of fluid,  $C'_\infty$  is the ambient concentration of fluid,  $\beta, \beta^*, u'_\infty$  and  $g$  are the coefficient of thermal expansion, coefficient of concentration

expansion, free steam velocity, and acceleration due to gravity, respectively.  $\sigma_0$  is the electrical conductivity,  $\rho$  is the fluid density,  $\nu$  is the kinematic viscosity,  $\mu$  is the dynamic viscosity,  $c_p$  is the specific heat at constant pressure of the fluid,  $b$  is the constant,  $Dis$  is the diffusion coefficient, and  $Kr'$  is the chemical reaction parameter.

Using the Rosseland approximation (Brewster), the radiative heat flux in  $y'$  direction is given by

$$q_r = -\frac{4\sigma^*}{3k^*} \frac{\partial T'^4}{\partial y'} \quad (7)$$

Here  $\sigma^*$  is the Stefan-Boltzmann constant, and  $k^*$  is the mean absorption coefficient. Using Eq. (7), the energy Eq. (4) becomes

$$u' \frac{\partial T'}{\partial x'} + v' \frac{\partial T'}{\partial y'} = \frac{k_e}{\rho c_p} \frac{\partial^2 T'}{\partial y'^2} + \frac{4\sigma^*}{3k^* \rho c_p} \frac{\partial^2 T'^4}{\partial y'^2} \quad (8)$$

It is convenient to make the governing equations and conditions dimensionless by using

$$\begin{aligned} x &= \frac{bx'}{u'_\infty}, y = \frac{by'}{u'_\infty}, R, u = \frac{u'}{u'_\infty}, \phi = \frac{C' - C'_\infty}{C'_w - C'_\infty}, \\ v &= \frac{v'}{u'_\infty}, R, R = \frac{u'_\infty}{\sqrt{cv}}, \theta = \frac{T' - T'_\infty}{T'_w - T'_\infty}, M = \frac{\sigma_0 B_0^2}{\rho b}, \\ Gr &= \frac{g\beta(T'_w - T'_\infty)}{bu'_\infty}, Gc = \frac{g\beta^*(C'_w - C'_\infty)}{bu'_\infty}, \\ Da^{-1} &= \frac{\nu}{Kb}, \gamma = \frac{C_1 u'_\infty}{b}, Pr = \frac{\mu c_p}{k}, F = \frac{kk^*}{4\sigma^* T_\infty^3}, \\ r &= \frac{T'_w - T'_\infty}{T'_\infty}, Sc = \frac{\nu}{D}, Kr = \frac{Kr'}{b}. \end{aligned} \quad (9)$$

where  $R$  is the Reynolds number.

In view of the Eq. (9), the Eqs. (1, 2, 3, 8 and 5) are reduced to the following non-dimensional form.

$$\frac{\partial u}{\partial x} + \frac{\partial v}{\partial y} = 0 \quad (10)$$

$$u \frac{\partial u}{\partial x} + v \frac{\partial u}{\partial y} = \frac{\partial^2 u}{\partial y^2} + Gr\theta + Gc\phi \quad (11)$$

$$+ N \frac{\partial \sigma}{\partial y} - \left( M + \frac{1}{Da} \right) u - \gamma u^2$$

$$G \frac{\partial^2 \sigma}{\partial y^2} - 2\sigma - \frac{\partial u}{\partial y} = 0 \quad (12)$$

$$u \frac{\partial \theta}{\partial x} + v \frac{\partial \theta}{\partial y} = \frac{1}{Pr} \frac{\partial^2 \theta}{\partial y^2}$$

$$+ \frac{4}{3F Pr} \left[ (1+r\theta)^3 \frac{\partial^2 \theta}{\partial y^2} + 3r(1+r\theta)^2 \left( \frac{\partial \theta}{\partial y} \right)^2 \right] \quad (13)$$

$$u \frac{\partial \phi}{\partial x} + v \frac{\partial \phi}{\partial y} = \frac{1}{Sc} \frac{\partial^2 \phi}{\partial y^2} - Kr\phi \quad (14)$$

The corresponding boundary conditions are

$$u = x, v = 0, \sigma = 0, \theta = 1, \phi = 1 \text{ at } y = 0,$$

$$u = 1, \sigma = 0, \theta = 0, \phi = 0 \text{ as } y \rightarrow \infty \quad (15)$$

Proceeding with the analysis, we define a stream function  $\psi(x, y)$  such that

$$u = \frac{\partial \psi}{\partial y}, v = -\frac{\partial \psi}{\partial x} \quad (16)$$

Now, let us consider the steam function as if

$$\psi(x, y) = f(y) + xg(y) \quad (17)$$

$$\sigma = xh(y) \quad (18)$$

In view of Eq. (16–18), the continuity Eq. (10) is identically satisfied and the momentum Eq. (11), angular momentum Eq. (12), energy Eq. (13), and species Eq. (14) become

$$\frac{\partial \psi}{\partial y} \frac{\partial^2 \psi}{\partial x \partial y} - \frac{\partial \psi}{\partial x} \frac{\partial^2 \psi}{\partial y^2} = \frac{\partial^3 \psi}{\partial y^3} + Gr\theta$$

$$+ Gc\phi - \left( M + \frac{1}{Da} \right) \frac{\partial \psi}{\partial y} + \gamma \left( \frac{\partial \psi}{\partial y} \right)^2 \quad (19)$$

$$G \frac{\partial^2 \sigma}{\partial y^2} - 2\sigma - \frac{\partial u}{\partial y} = 0 \quad (20)$$

$$\frac{\partial \psi}{\partial y} \frac{\partial \theta}{\partial x} - \frac{\partial \psi}{\partial x} \frac{\partial \theta}{\partial y} = \frac{1}{Pr} \frac{\partial^2 \theta}{\partial y^2} + \frac{4}{3F Pr} \left[ (1+r\theta)^3 \frac{\partial^2 \theta}{\partial y^2} + 3r(1+r\theta)^2 \left( \frac{\partial \theta}{\partial y} \right)^2 \right] \quad (21)$$

$$\frac{\partial \psi}{\partial y} \frac{\partial \phi}{\partial x} - \frac{\partial \psi}{\partial x} \frac{\partial \phi}{\partial y} = \frac{1}{Sc} \frac{\partial^2 \phi}{\partial y^2} - Kr\phi \quad (22)$$

and the boundary conditions (15) become

$$\frac{\partial \psi}{\partial y} = x, \frac{\partial \psi}{\partial x} = 0, h = 0, \theta = 1, \phi = 1 \text{ at } y = 0$$

$$\frac{\partial \psi}{\partial y} \rightarrow 1, h \rightarrow 0, \theta \rightarrow 0, \phi \rightarrow 0 \text{ as } y \rightarrow \infty \quad (23)$$

In Eqs. (19, 20, 21, 22) and equating coefficient of  $x^0$  and  $x^1$ , we obtain the coupled non-linear ordinary differential equations

$$f''' + f''g - f'g' - \left( M + \frac{1}{Da} \right) f' \quad (24)$$

$$-\gamma f'^2 + Gr\theta + Gc\phi = 0$$

$$g''' + gg'' - (g')^2 - \left( M + \frac{1}{Da} \right) g' \quad (25)$$

$$-2\gamma f'g' + Nh' = 0$$

$$Gh'' - 2h - g'' = 0 \quad (26)$$

$$\left( 3F + 4(1+r\theta)^3 \right) \theta'' + 3Pr Fg\theta' \quad (27)$$

$$+ 12r(1+r\theta)^2 \theta'^2 = 0$$

$$\phi'' + Scg\phi' - KrSc\phi = 0 \quad (28)$$

where a prime denotes differentiation with respect to  $y$ .

In view of Eqs. (17, 18), the boundary condition (23) reduce to

$$f = 0, f' = 0, g = 0, g' = 1, h = 1, \theta = 1,$$

$$\phi = 1 \text{ at } y = 0$$

$$f' \rightarrow 1, g' \rightarrow 0, h \rightarrow 0, \theta \rightarrow 0, \phi \rightarrow 0 \text{ as } y \rightarrow \infty \quad (29)$$

The physical quantities which are of importance for this problem are the skin-friction coefficient, Nusselt number and Sherwood number, which are defined by

The shear stress at the stretching surface is given by

$$\begin{aligned} \tau_w &= (\mu + k) \left( \frac{\partial u'}{\partial y'} \right)_{y'=0} + k(\sigma)_{y'=0} \\ &= \rho \nu bR \left( \frac{\partial u}{\partial y} \right)_{y=0} \\ &= \rho \nu bR (f''(0) + xg''(0)) \end{aligned} \quad (30)$$

The skin-friction coefficient

$$C_f = \frac{\tau_w}{\frac{1}{2} \rho u_\infty^2} = \frac{2}{R} (f''(0) + xg''(0)) \quad (31)$$

The wall heat flux is given by

$$\begin{aligned} q_w &= -k \left( \frac{\partial T'}{\partial y'} \right)_{y'=0} = -k \frac{bR}{u_\infty} \left( \frac{\partial T}{\partial y} \right)_{y=0} \\ &= -k \frac{bR}{u_\infty} (T'_w - T'_\infty) \theta'(0) \end{aligned} \quad (32)$$

Nusselt number

$$Nu = \frac{q_w}{k(T'_w - T'_\infty)} = \frac{bR}{u_\infty} \theta'(0) \quad (33)$$

The wall mass flux is given by

$$\begin{aligned} m_w &= -D \left( \frac{\partial C'}{\partial y'} \right)_{y'=0} = -D \frac{bR}{u_\infty} \left( \frac{\partial C}{\partial y} \right)_{y=0} \\ &= -D \frac{bR}{u_\infty} (C'_w - C'_\infty) \phi'(0) \end{aligned} \quad (34)$$

Sherwood number

$$Sh = \frac{m_w}{D(C'_w - C'_\infty)} = \frac{bR}{u_\infty} \phi'(0) \quad (35)$$

### 3. Solution of the problem

The shooting method for linear equations is based on replacing the boundary value problem by two initial value problems and the solution of the boundary value problem is a linear combination between the solutions of the two initial value problems. The shooting method for the nonlinear boundary value problem is similar to the linear case, except that the solution of the nonlinear problem cannot be simply expressed as a linear combination of the solutions of the two initial value problems. Instead, we need to

use a sequence of suitable initial values for the derivatives such that the tolerance at the end point of the range is very small. This sequence of initial values is given by the second method, and we use the fourth order Runge-Kutta method to solve the initial value problems. The full Eqs. (24–28) with the boundary conditions (29) were solved numerically using the Runge-Kutta method algorithm with a systematic guessing  $f''(0), g''(0), h'(0), \theta'(0)$  and  $\phi'(0)$  by the shooting technique until the boundary conditions at infinity  $f'(y)$  decay exponentially to one, also  $g'(0), h(y), \theta(y)$  and  $\phi(y)$  to zero. The functions  $f', g', -h, \theta$  and  $\phi$  are shown in figures.

#### 4. Results and discussion

As a result of the numerical calculations, the dimensionless velocity, angular velocity, temperature, and concentration distributions for the flow under consideration were obtained. Also their behavior were discussed for variations in the governing parameters, namely, the thermal Grashof number  $Gr$ , solutal Grashof number  $Gc$ , magnetic field parameter  $M$ , Darcy number  $Da$ , porous medium inertia coefficient  $\gamma$ , vorticity viscosity parameter  $N$ , micro-rotation parameter  $G$ , Prandtl number  $Pr$ , radiation parameter  $F$ , the parameter of relative difference between the temperature of the sheet and temperature far  $r$ , Eckert number  $Ec$ , Schmidt number  $Sc$ , and chemical reaction parameter  $Kr$ . In the present study, the following default parametric values are adopted:  $Gr = 1.0, Gc = 1.0, M = 0.01, Da = 100, \gamma = 0.1, N = 0.1, G = 2.0, Pr = 0.71, F = 1.0, r = 0.05, Sc = 0.6, Kr = 0.5$ . in all graphs. Therefore, corresponding values of these parameters are same, unless they are specifically indicated on the appropriate graphs. Figure 2(a) shows the variation of the dimensionless velocity component  $f'$  for several sets of values of thermal Grashof number  $Gr$ . As expected, it is observed that there is a rise in the velocity due to the enhancement of thermal buoyancy force. The variation of the dimensionless velocity component  $f'$  for several sets of values of solutal Grashof number  $Gc$  is depicted in Fig. 2(b). As expected, the fluid velocity increases and the

peak value is more distinctive due to the increase in the species buoyancy force. It should be mentioned herein that the profiles of  $g', h, \theta$  and  $\phi$  were found to be insensible to change in  $Gr$  and  $Gc$ , therefore, not shown herein for brevity. The accuracy of the aforementioned numerical method was also validated by direct comparison with the numerical results reported by Abo-Eldehbab and El-Aziz [47] in Fig. 1 and as well as table 1. Figure 1 represents the comparison of angular velocity profiles and Table 1 presents comparisons of the velocities of  $f''(0)$  and  $g''(0)$  values for various  $M$  values. These comparisons show an excellent agreement between the results.

The effect of variation of the magnetic parameter  $M$  on the velocities ( $f'$  and  $g'$ ), angular velocity  $-h$ , temperature  $\theta$ , and concentration  $\phi$  profiles is presented in Figs. 3(a-e), respectively. It is well known that the application of a uniform magnetic field normal to the flow direction gives rise to a force called Lorentz. This force has the tendency to slow down the velocity of the fluid and angular velocity of micro-rotation in the boundary layer and to increase its temperature and concentration. This is obvious from the decreases in the velocity profiles and angular velocity of micro-rotation profiles while temperature and concentration profiles increase. Figures 3(a-e) present typical profiles for the variables of the fluid's  $x$ -component of velocities ( $f'$  and  $g'$ ), angular velocity  $-h$ , temperature  $\theta$ , and concentration  $\phi$  for different values of Hartmann number. It is noted that as the value of  $M$  increases, the fluid velocities, angular velocity, and temperature decrease, whereas the concentration of the fluid increases. Figures 4(a-e) present typical profiles for the variables of the fluid's  $x$ -component of velocities ( $f'$  and  $g'$ ), angular velocity  $-h$ , temperature  $\theta$ , and concentration  $\phi$  for different values of Darcy number  $Da$ . It is noted that as the value of  $Da$  increases, the fluid velocities and angular velocity increase while temperature and concentration of the fluid decrease. Figures 5(a-e) present the typical profiles for the variables of the fluid's  $x$ -component of velocities ( $f'$  and  $g'$ ), angular velocity  $-h$ , temperature  $\theta$ , and

concentration  $\phi$  for different values of the porous medium inertia coefficient  $\gamma$ . Obviously, the porous medium inertia effects constitute resistance to the flow. Thus as the inertia coefficient increases, the resistance to the flow increases, causing the fluid flow in the porous medium to slow down, and temperature as well as concentration increase. Therefore, as  $\gamma$  increases,  $f'$ ,  $g'$ , and  $-h$  decrease while the temperature  $\theta$  and concentration  $\phi$  increase. Figures 6(a–e) present the typical profiles for the variables of the fluid's  $x$ -component of velocities ( $f'$  and  $g'$ ), angular velocity  $-h$ , temperature  $\theta$ , and concentration  $\phi$  for different values of the vortex viscosity parameter  $N$ . Increases in the values of  $N$  have a tendency to increase  $f'$ ,  $-h$ ,  $\theta$ , and  $\phi$  and to decrease  $g'$ . Figure 7 is a plot of the dimensionless angular velocity  $-h$  profiles for different values of the micro-rotation parameter  $G$ . The curves illustrate that, as the values of  $G$  increase, the angular velocity  $-h$ , as expected, decreases with an increase in the boundary layer thickness as the maximum moves away from the sheet. Of course, when the viscosity of the fluid decreases the angular velocity of additive increases. Figure 8(a) illustrates the dimensionless velocity component  $f'$  for different values of the Prandtl number  $Pr$ . The numerical results show that the effect of increasing values of the Prandtl number results in a decreasing velocity. From Fig. 8(b), it is observed that an increase in the Prandtl number results in a decrease in the thermal boundary layer thickness and in general lowers average temperature within the boundary layer. The reason is that smaller values of  $Pr$  are equivalent to increasing the thermal conductivities. Therefore, heat is able to diffuse away from the heated plate more rapidly than for higher values of  $Pr$ . Hence in the case of smaller Prandtl numbers, as the boundary layer is thicker, the rate of heat transfer is reduced. The effect of the radiation parameter  $F$  on the dimensionless velocity component  $f'$  and dimensionless temperature is shown in Figs. 9(a and b), respectively. Figure 9(a) shows that velocity component  $f'$  decreases with an increase in the radiation parameter  $F$ . From Fig.

9(b) it is seen that the temperature decreases as the radiation parameter  $F$  increases. This result qualitatively agrees with expectations, since the effect of radiation is to decrease the rate of energy transport to the fluid, thereby decreasing the temperature of the fluid.

The influence of parameter of the relative difference between the temperature of the sheet and the temperature far away from the sheet  $r$  on dimensionless velocity  $f'$  and temperature profiles are plotted in Figs. 10(a and b), respectively. Figure 10(a) shows that the dimensionless velocity  $f'$  increases with an increase in  $r$ . It is observed that the temperature increases with an increase in  $r$  (Fig. 10(b)). The influence of the Schmidt number  $Sc$  on the dimensionless velocity  $f'$  and concentration profiles is plotted in Figs. 11(a and b), respectively. As the Schmidt number increases, the concentration decreases. This causes the concentration buoyancy effects to decrease, yielding suction in the fluid velocity. The reductions in the velocity and concentration profiles are accompanied by simultaneous reductions in the velocity and concentration boundary layers. These behaviors are clear from Figs. 11(a and b). The effects of the chemical reaction parameter  $Kr$  on dimensionless velocity component  $f'$  and concentration profiles are plotted in Figs. 12 (a and b), respectively. As the chemical reaction parameter increases, the velocity and concentration profiles decrease. These behaviors are clear from Figs. 12 (a and b). Tables 2 - 4 provide the missing wall functions for velocity, angular velocity, temperature, and concentration functions. These quantities are useful in the evaluation of wall shear stresses, the gradient of angular velocity, surface heat transfer rate, and mass transfer rate. The results are obtained for  $r = 0.05$  and different values of the thermal Grashof number  $Gr$ , solutal Grashof number  $Gc$ , magnetic field parameter  $M$ , Darcy number  $Da$ , porous medium inertia coefficient  $\gamma$ , vortex viscosity parameter  $N$ , micro-rotation parameter  $G$ , radiation parameter  $F$ , the parameter of relative difference between the temperature of the sheet and temperature far away from the sheet  $r$ , Prandtl number  $Pr$ , and Schmidt number  $Sc$ . Table 2

indicates that increasing the values of the Grashof number  $Gr$  and solutal Grashof number  $Gc$  results in an increase in the value of  $f''(0)$ . This is because as  $Gr$  and  $Gc$  increase, the momentum boundary layer thickness decreases and, therefore, an increase in the value of  $f''(0)$  occurs. The results indicate that a distinct fall in the skin-friction coefficient in the  $x$ -direction ( $f''(0)$  and  $g''(0)$ ), the surface heat transfer rate  $-\theta'(0)$ , and mass transfer rate  $-\phi'(0)$ , accompanies a rise in the magnetic field parameter  $M$  when the gradient of angular velocity  $h'(0)$  increases. Increasing the value of  $Da$  has the effect of an increase in the skin-friction function  $f''(0)$ , heat transfer rate  $-\theta'(0)$ , and mass transfer rate  $-\phi'(0)$ . Where as the gradient of angular velocity  $h'(0)$  and the skin-friction function  $g''(0)$  slightly decrease as  $Da$  increases. Furthermore, the influence of the porous medium inertia coefficient on the wall shear stresses, the gradient of angular velocity, surface heat transfer, and surface mass transfer rate is the same as that of the inverse Darcy number  $Da$ , since it also represents resistance to the flow. Namely, as  $\gamma$  increases,  $f''(0)$ ,  $\theta'(0)$ ,  $\phi'(0)$  decrease while  $g''(0)$ ,  $h'(0)$  slightly increases. From Table 3 for given values of  $Gr$ ,  $Gc$ ,  $M$ ,  $Da$ ,  $\gamma$ ,  $Sc$  and  $Kr$ , it can be found that increasing the value of micro-rotation parameter  $N$  reduces the skin-friction function  $g''(0)$ ,  $\theta'(0)$  and  $\phi'(0)$ , while the skin-friction function  $f''(0)$  and the gradient of angular velocity  $h'(0)$  increase as  $N$  increases. The skin friction  $f''(0)$  increases and the gradient of angular velocity  $h'(0)$  decreases as the micro-rotation parameter  $G$  increases, while the skin-friction coefficient in the  $x$ -directions  $g''(0)$ , heat transfer rate  $-\theta'(0)$ , and mass transfer rate  $-\phi'(0)$  are insensible to the change in  $G$ . It is observed that the magnitude of the wall temperature gradient increases as Prandtl number  $Pr$  or radiation parameter  $F$  increase. From Table 4, the magnitude of the wall concentration increases with an increase in the Schmidt number  $Sc$  or chemical reaction parameter  $Kr$ . Furthermore, the negative values of the wall temperature and concentration gradients, for all values of the dimensionless parameters, are indicative of the physical fact

that the heat flows from the sheet surface to the ambient fluid.

### 5. Conclusions

The problem of steady, laminar, free convection boundary layer flow of micropolar fluid from a vertical stretching surface embedded in a non-Darcian porous medium in the presence of thermal radiation, mass transfer, uniform magnetic field, chemical reaction, and free stream velocity was investigated. A similar transformation was employed to change the governing partial differential equations into ordinary one. These equations were solved numerically by the fourth order Rung-Kutta along with the shooting technique. A wide selection of numerical results was presented giving the evolution of the velocity, micro-rotation, temperature, and concentration profiles as well as the skin- friction coefficient, heat transfer rate, and mass transfer rate. It was found that the skin-friction coefficient, heat transfer rate, and mass transfer rate decrease and the gradient of angular velocity increases as the inverse Darcy number, porous medium inertia coefficient, or magnetic field parameter increase. Increases in the heat generation/absorption coefficient increased the skin-friction coefficient and decreased the heat transfer rate. It was noticed that the increase in radiation parameter or Prandtl number caused a decrease in the skin-friction coefficient and an increase in heat transfer rate. In addition, it was found that the increase in Schmidt number and chemical reaction caused a decrease in skin-friction coefficient and an increase in mass transfer rate.

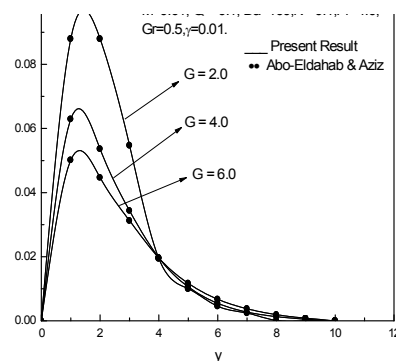


Fig. 1. Comparison of angular velocity Profiles.

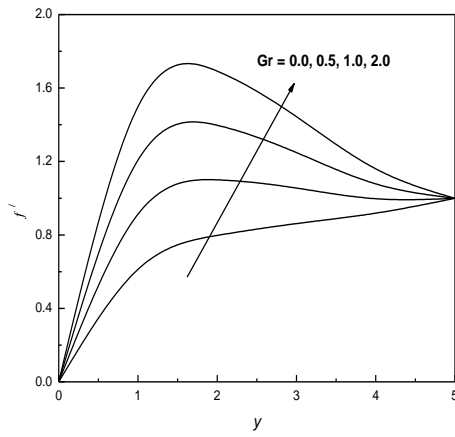


Fig. 2(a). Variation of the velocity component  $f'$  with  $Gr$ .

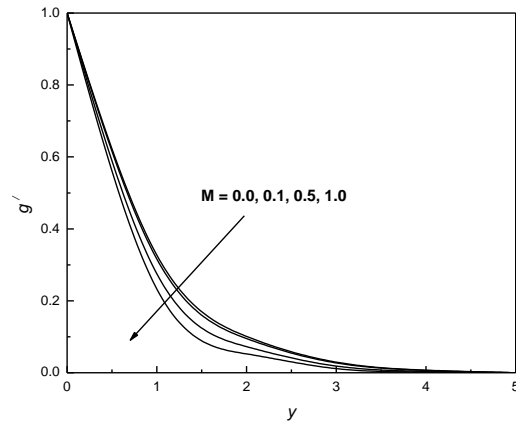


Fig. 3(b). Variation of the velocity component  $g'$  with  $M$ .

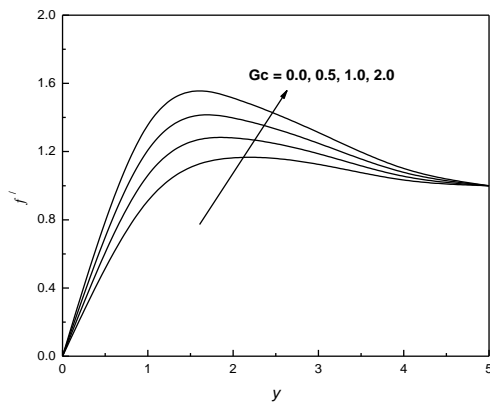


Fig. 2(b). Variation of the velocity component  $f'$  with  $Gc$ .

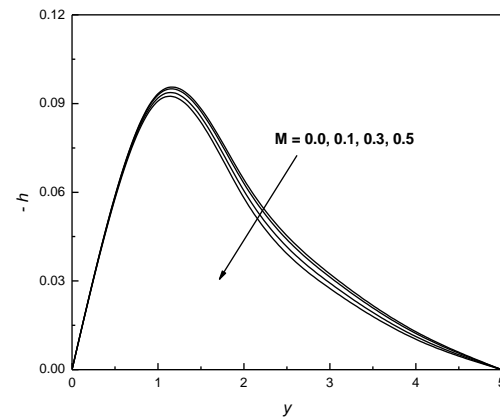


Fig. 3(c). Variation of the velocity component  $-h$  with  $M$ .

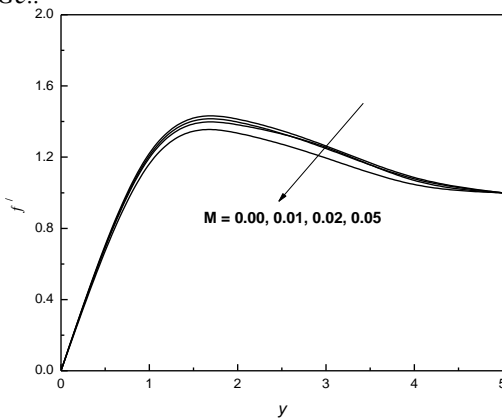


Fig. 3(a). Variation of the velocity component  $f'$  with  $M$ .

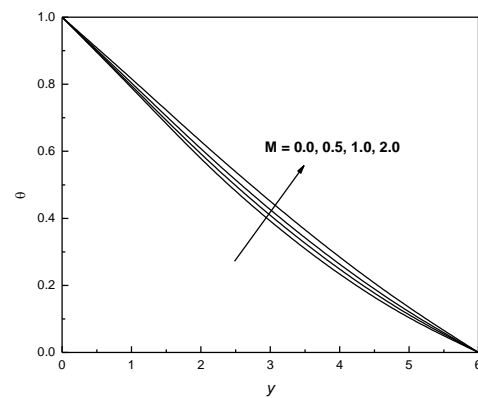
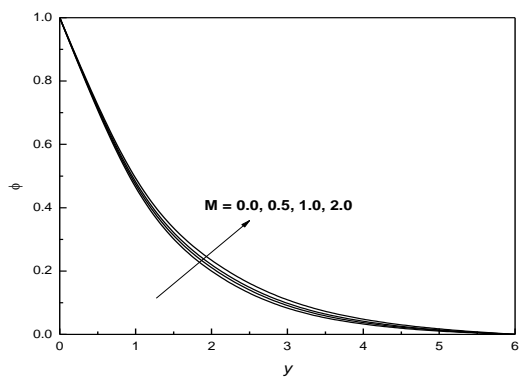
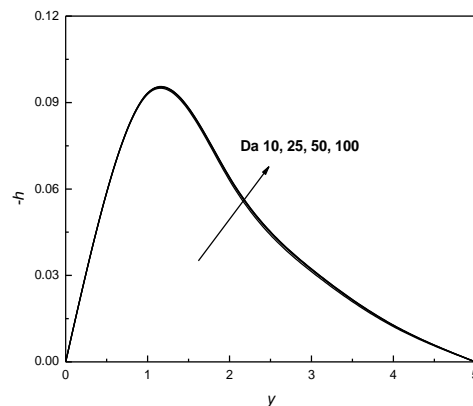


Fig. 3(d). Variation of the velocity component  $\theta$  with  $M$ .



**Fig. 3(e).** Variation of the velocity component  $\phi$  with  $M$ .



**Fig. 4(c).** Variation of the velocity component  $-h$  with  $Da$ .

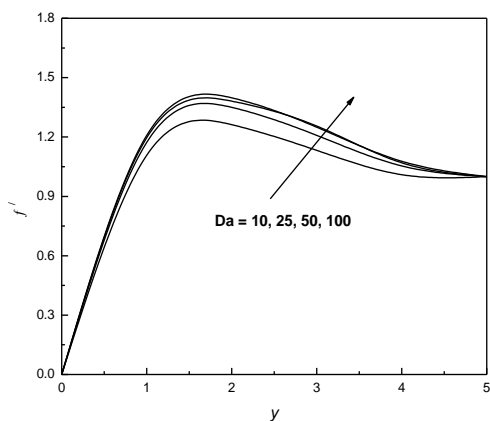


**Fig. 4(a).** Variation of the velocity component  $f'$  with  $Da$ .

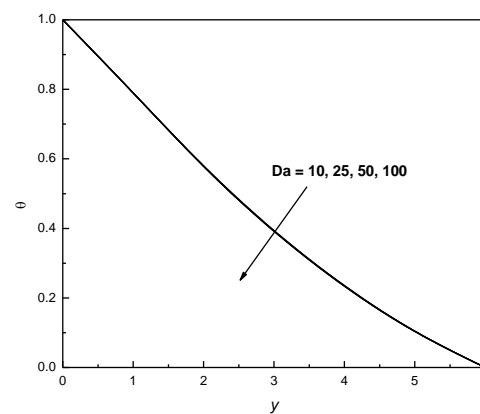


**Fig. 4(d).** Variation of the velocity component  $\theta$  with  $Da$ .

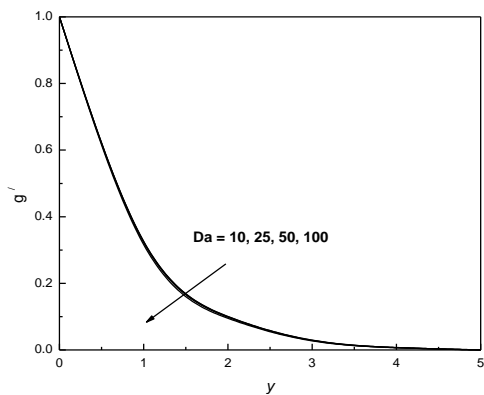


**Fig. 4(b).** Variation of the velocity component  $g'$  with  $Da$ .

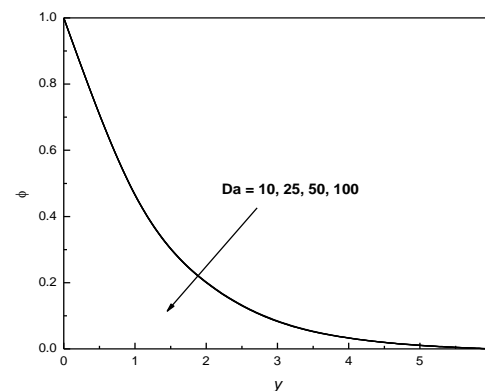


**Fig. 4(e).** Variation of the velocity component  $\phi$  with  $Da$ .

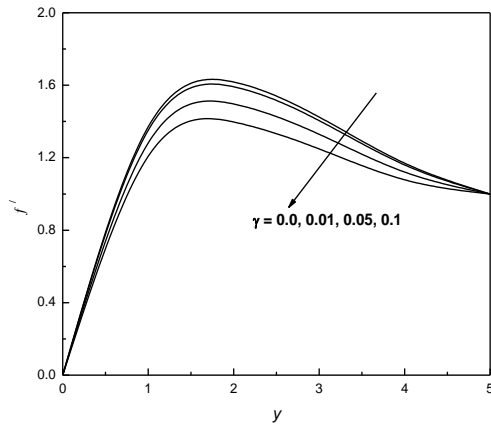


**Fig. 5(a).** Variation of the velocity component  $f'$  with  $\gamma$ .

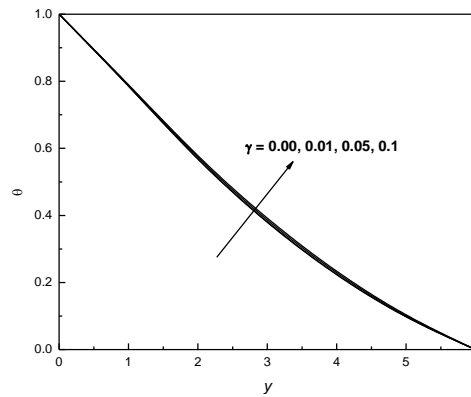


**Fig. 5(d).** Variation of the velocity component  $\theta$  with  $\gamma$ .

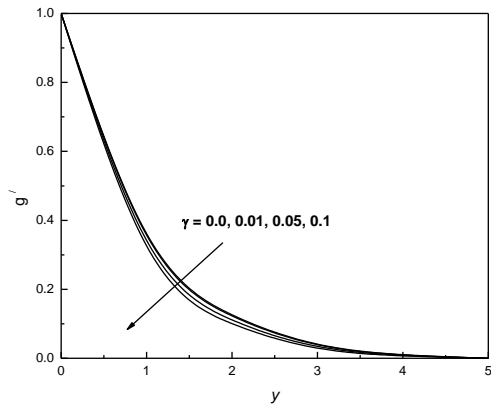


**Fig. 5(b).** Variation of the velocity component  $g'$  with  $\gamma$ .

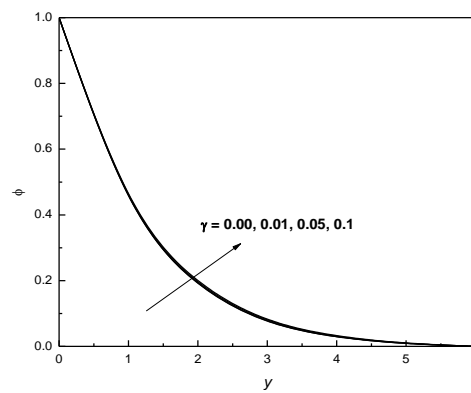


**Fig. 5(e).** Variation of the velocity component  $\phi$  with  $\gamma$ .

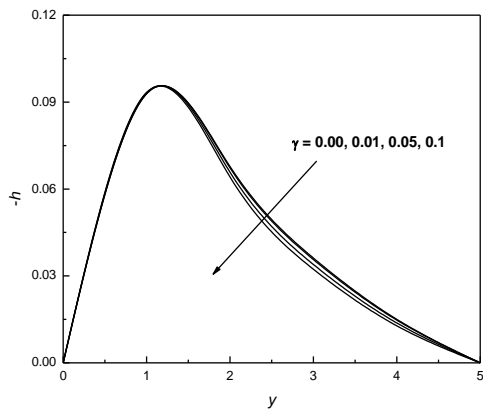


**Fig. 5(c).** Variation of the velocity component  $-h$  with  $\gamma$ .

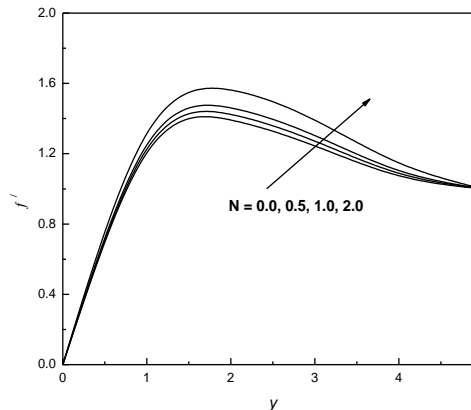


**Fig. 6(a).** Variation of the velocity component  $f'$  with  $N$

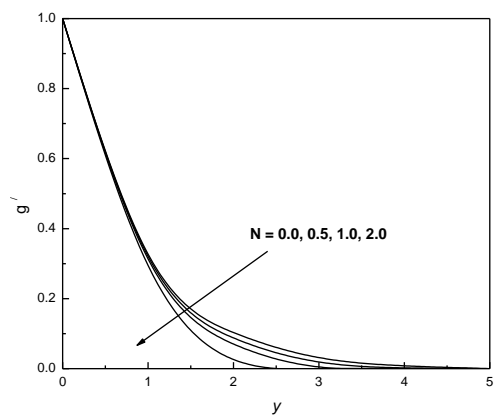


**Fig. 6(b).** Variation of the velocity component  $g'$  with  $N$ .

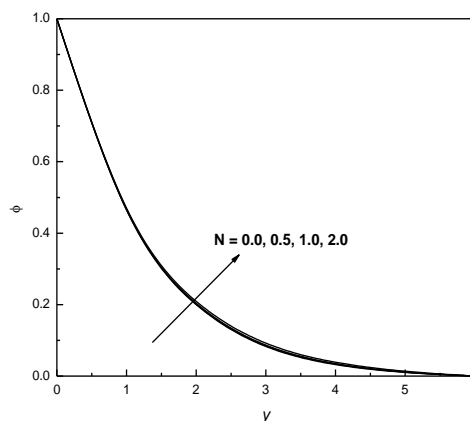


**Fig. 6(e).** Variation of the velocity component  $\phi$  with  $N$ .

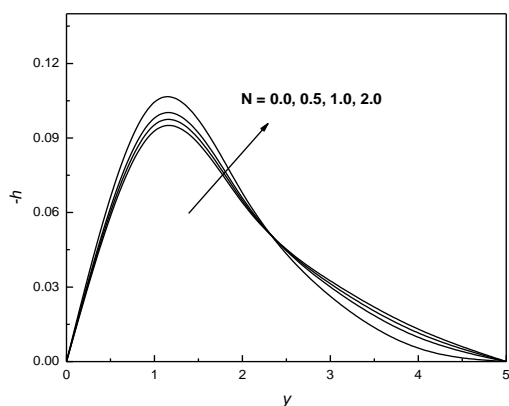


**Fig. 6(c).** Variation of the velocity component  $-h$  with  $N$ .

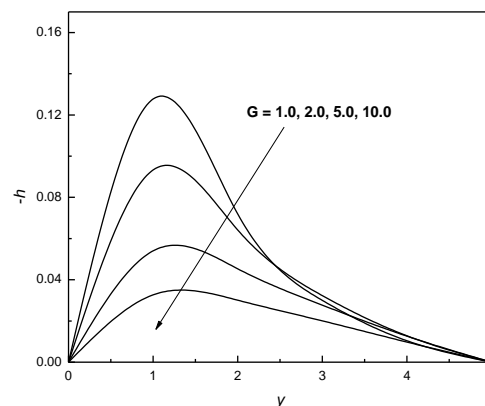


**Fig. 7.** Variation of the velocity component  $-h$  with  $G$ .

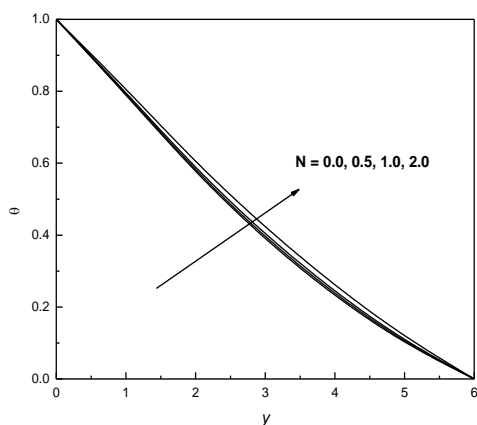


**Fig. 6(d).** Variation of the velocity component  $\theta$  with  $N$ .

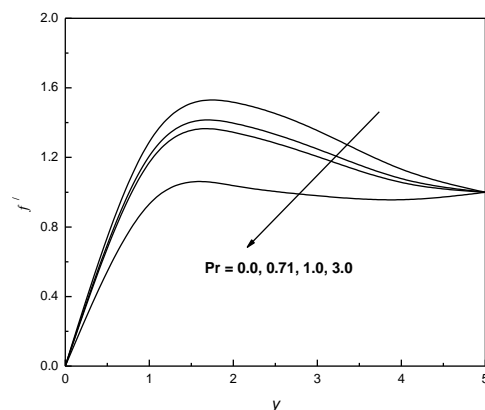


**Fig. 8(a).** Variation of the velocity component  $f'$  with  $Pr$ .

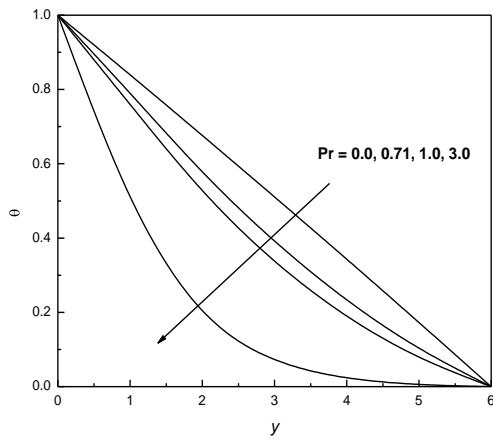


**Fig. 8(b).** Variation of the velocity component  $\theta$  with  $Pr$ .

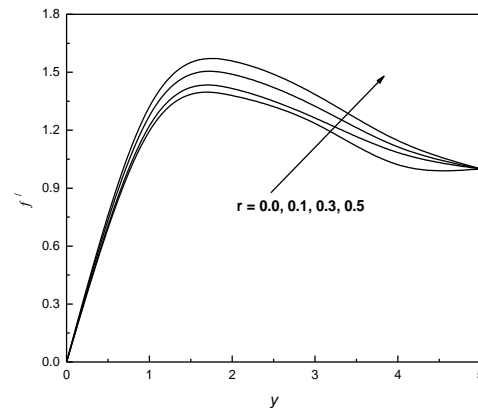


**Fig. 10(a).** Variation of the velocity component  $f'$  with  $r$ .

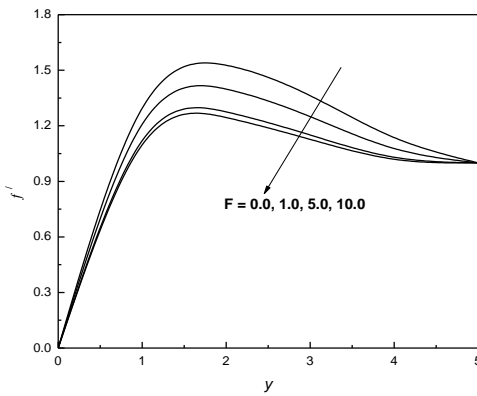


**Fig. 9(a).** Variation of the velocity component  $f'$  with  $F$ .

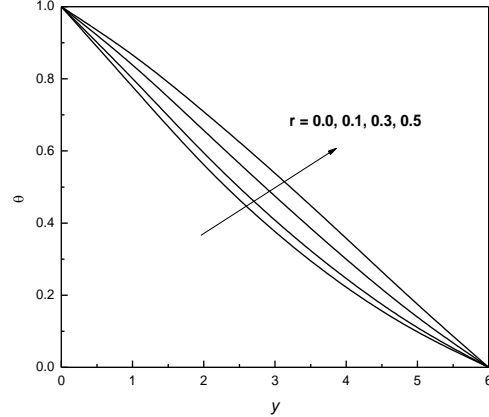


**Fig. 10(b).** Variation of the velocity component  $\theta$  with  $r$ .

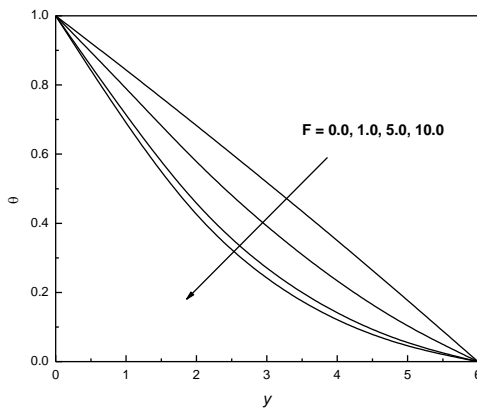


**Fig. 9(b).** Variation of the velocity component  $\theta$  with  $F$ .

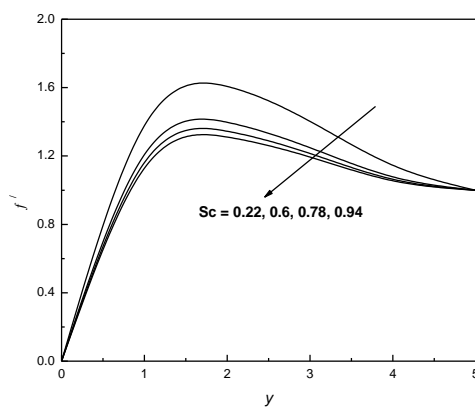


**Fig. 11(a).** Variation of the velocity component  $f'$  with  $Sc$ .

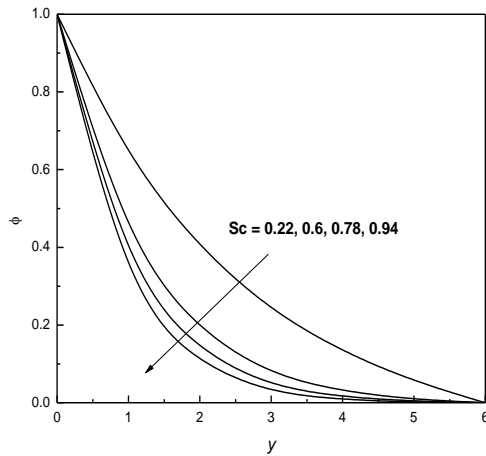


Fig. 11(b). Variation of the velocity component  $\phi$  with  $Sc$ .

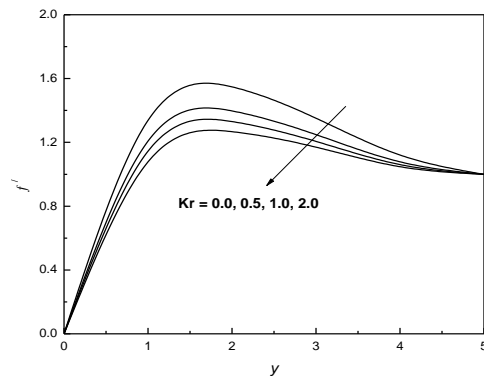


Fig. 12(a). Variation of the velocity component  $f'$  with  $Kr$ .

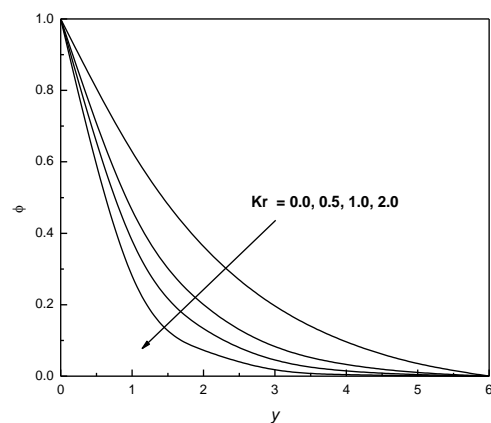


Fig. 12(b). Variation of the velocity component  $\phi$  with  $Kr$ .

References

[1] A. C. Eringen, “Theory of micropolar fluids”, *Journal of Mathematics and Mechanics*, Vol. 16, pp. 1-18, (1966).

[2] T. Y. Na, and I. Pop, “Boundary-layer flow of micropolar fluid due to a stretching wall”, *Archives of Applied Mechanics*, Vol. 67, No. 4, pp. 229-236, (1977).

[3] A. Desseaux, and N. A. Kelson, “Flow of a micropolar fluid bounded by a stretching sheet”, *Anziam J.*, Vol. 42, pp. 536-560, (2000).

[4] F. M. Hady, On the solution of heat transfer to micropolar fluid from a non-isothermal stretching sheet with injection, *Int. J. Numer. Methods for Heat and Fluid Flow*, Vol. 6, No. 6, pp. 99-104, (1966).

[5] O. Aydin and A. Kaya, “Non-Darcin forced convection flow of a viscous dissipating fluid over a flat plate embedded in a porous medium”, *Trans Porous Media*, Vol. 73, No. 2, pp. 173-186, (2008).

[6] S. S. Das, A. Satapathy, J. K. Das and J. P. Panda, “Mass transfer effects on MHD flow and heat transfer past a vertical porous plate through a porous medium under oscillatory suction and heat source”, *Int. J. of Heat and Mass Transfer.*, Vol. 52, No. 25-26, pp. 5962-5969, (2009).

[7] J. Anand Rao and S. Shivaiah, “Chemical reaction effects on an unsteady MHD free convective flow past an infinite vertical porous plate with constant suction and heat source”, *Int. J. of Appl. Math and Mech.*, Vol. 7, No. 8, pp. 98-118,(2011).

[8] S. Y. Ibrahim and O. D. Makinde, “Radiation effect on chemically reacting magneto hydrodynamics (MHD) boundary layer flow of heat and mass transfer through a porous vertical flat plate,” *Int. J. Physical Sciences*, Vol. 6, No. 6, pp. 1508-1516, (2011).

[9] D. Pal and B. Talukdar, “Combined effects of Joule heating and chemical

- reaction on unsteady magneto hydrodynamic mixed convection of a viscous dissipating fluid over a vertical plate in porous media with thermal radiation,” *Mathematical and Computer Modelling*, Vol. 54, No. 11-12, pp. 3016-3036, (2011).
- [10] K. Jhansi Rani and Ch. V. Ramana Murthy, “MHD Flow over a Moving Infinite Vertical Porous Plate with Uniform Heat Flux in the presence of Thermal Radiation”, *Advanced in Theoretical and Applied Mathematics*, Vol. 6, No. 1, pp. 51-63, (2011).
- [11] G. V. Ramana Reddy, N. Bhaskar Reddy and Ch. V. Ramana Murthy, “Heat and mass transfer effects on MHD free convection flow past an oscillating plate embedded in porous medium”, *International Journal of Physical Sciences*, Vol. 22. No. 2M, pp. 375-380, (2010).
- [12] T. S. Reddy, M. C. Raju and S. V. K. V Varma “ unsteady MHD Radiative and Chemically reactive free convection flow near a moving vertical plate in porous medium” *Journal of Applied Fluid Mechanics* ,Vol. 6, No. 3, pp. 443-451, (2013).
- [13] M. C. Raju, S. V. K. Varma, N. A. Reddy, “MHD Thermal diffusion natural convection flow between heated inclined plates in porous medium”, *Journal on future engineering and technology*, Vol. 6, No. 2, pp. 45-48, (2011).
- [14] P.Chandrakala, “Radiation Effects on Flow Past an Impulsively Started Vertical Oscillating Plate with Uniform Heat Flux”, *International Journal of Dynamics of Fluids*, Vol. 7, No. 1, pp. 1-8, (2011).
- [15] R. Choudhury and U. J. Das, “MHD mixed convective heat and mass transfer in a viscoelastic boundary layer slip flow past a vertical permeable plate with thermal radiation and chemical reaction”, *Int. J. of statistika and matematika*, Vol. 3, No. 3, pp. 93-101, (2012).
- [16] S. Abzal, G. R. Reddy and S. V. K. Varma, “MHD free convection flow and mass transfer unsteady near a moving vertical plate in the presence of thermal radiation”, *Annals of faculty engineering hunedoara-International journal of engineering*, Tom IX, pp. 29-34, (2011).
- [17] V. Ravikumar, M. C. Raju and G. S. S. Raju, “Magnetic field and radiation effects on a double diffusive free convective flow bounded by two infinite impermeable plates in the presence of chemical reaction”, *IJSER*, Vol. 4, No. 7, pp. 1915-1923, (2013).
- [18] R. A. Mohamed, Abdel-Nasser A. Osman, S.M. Abo-Dahab, “Unsteady MHD double diffusive convection boundary-layer flow past a radiate hot vertical surface in porous media in the presence of chemical reaction and heat sink”, *Meccanica*, Vol. 48, No. 4, pp 931-942, (2013).
- [19] M. Y. Malik, T. Salahuddin, Arif Hussain and S Bilal, “MHD flow of tangent hyperbolic fluid over a stretching cylinder: Using Keller box method”, *Journal of Magnetism and Magnetic Materials*, Vol. 395, pp. 271-276, (2015).
- [20] T. Salahuddin, M. Y. Malik, Arif Hussain, S. Bilal and M. Awais, “The effects of transverse magnetic field with variable thermal conductivity on tangent hyperbolic fluid with exponentially varying viscosity”, *AIP Advances*, Vol. 5, Article ID: 127103, (2015).
- [21] T. Salahuddin, Md. Yousaf Malik, Arif Hussain and M. Awais, “MHD flow of Cattaneo-Christov heat flux model for Williamson fluid over a stretching sheet with variable thickness: Using numerical approach”, *Journal of Magnetism and Magnetic Materials*, Vol. 401, pp. 991-997, (2015).
- [22] B. Seshaiiah, S. V. K. Varma, M. C. Raju, “The effects of chemical reaction and radiation on unsteady MHD free convective fluid flow embedded in a porous medium with time-dependent suction with temperature gradient heat source”, *International Journal of Scientific Knowledge*, Vol. 3 No. 2, pp. 13-24, (2013).

- [23] R. Rout and H. B. Pattanayak, "Chemical reaction and radiation effects on MHD flow past an exponentially accelerated vertical plate in presence of heat source with variable temperature embedded in a porous medium", *Annals of faculty engineering hunedoara- Int. Jou. Of Engg*, Vol. 4, pp. 253-259, (2013).
- [24] W. A. Khan, and I. Pop, "The Cheng-Minkowycz problem for the triple-diffusive natural convection boundary layer flow past a vertical plate in a porous medium", *J. Porous Media*, Vol. 16, No. 7, pp. 637-646, (2013).
- [25] G. S. Seth, R. Nandkeolyar and M. S. Ansari, "Effects of thermal radiation and rotation on unsteady hydro magnetic free convection flow past an impulsively moving vertical plate with ramped temperature in a porous medium", *J. Appl. Fluid Mech*, Vol. 6, No.1, pp. 27-38, (2013).
- [26] D. Ch. Kesavaiah, P. V. Satyanarayana, S. Venkataramana, "Effects of the chemical reaction and radiation absorption on an unsteady MHD convective heat and mass transfer flow past a semi-infinite vertical permeable moving plate embedded in a porous medium with heat source and suction", *Int. J. of Appl. Math and Mech.*, Vol. 7, No. 1, pp. 52-69, (2011).
- [27] U. S. Rajput, S. Kumar, "Radiation effects on MHD flow past an impulsively started vertical plate with variable heat and mass transfer", *Int. J. of Appl. Math. and Mech.*, Vol. 8, No. 1, pp. 66-85, (2012).
- [28] R. Muthucumaraswamy, N. Dhanasekar, G. Easwara Prasad, "Effects on first order chemical reaction on flow past an accelerated isothermal vertical plate in a rotating fluid with variable mass diffusion", *Int. J. Math.*, Vol. 4, No. 41, pp. 28-35, (2013).
- [29] B. Devika, P. V. Satya Narayana, S. Venkataramana, "MHD oscillatory flow of a visco elastic fluid in a porous channel with chemical reaction", *Int. J. Engg. Sci. Inv.*, Vol. 2, No. 2, pp. 26-35, (2013).
- [30] K. Chand, K. D. Singh, S. Kumar, "Hall effect on radiating and chemically reacting MHD oscillatory flow in a rotating porous vertical channel in slip flow regime", *Advances in Applied Sciences Research*, Vol. 3, No. 4, pp. 2424-2437, (2012).
- [31] S. Mukhopadhyay, R. S. R. Gorla, "Effects of partial slip on boundary layer flow past a permeable exponential stretching sheet in presence of thermal radiation", *Heat Mass Transfer*, Vol. 48, pp. 1773-1781, (2012). <http://dx.doi.org/10.1007/s00231-012-1024-8>.
- [32] P. K. Kameswaran, S. Shaw, P. Sibanda, P. V. S. N. Murthy, "Homogeneous-heterogeneous reactions in a nanofluid flow due to a porous stretching sheet", *Int. J. Heat and Mass Transfer*, Vol. 57, No. 2, pp. 465-472 (2013).
- [33] S. Shaw, P.K. Kameswaran, P. Sibanda, "Homogeneous-heterogeneous reactions in micropolar fluid flow from a permeable stretching or shrinking sheet in a porous medium", *Boundary Value Problems*, Vol. 77, No. 1, (2013).
- [34] R. Ellahi, S. Aziz, A. Zeeshan, "Non-Newtonian nanofluid flow through a porous medium between two coaxial cylinders with heat transfer and variable viscosity", *Journal of Porous Media*, Vol. 16, No. 1, pp. 205-216, (2013).
- [35] N. Bachok, A. Ishak, I. Pop, "Boundary layer stagnation-point flow and heat transfer over an exponentially stretching/shrinking sheet in a nanofluid", *Int. J. f Heat Mass transfer*, Vol. 55, No. 25-26, pp. 8122-8128, (2013).
- [36] N. S. Akbar, S. Nadeem, R.U. Haq, Z.H. Khan, "Radiation effects on MHD stagnation point flow of nanofluid towards a stretching surface with convective boundary condition", *Chinese Journal of Aeronautics*, Vol. 26, No. 6, pp. 1389-1397, (2013), DOI: <http://dx.doi.org/10.1016/j.cja.2013.10.008>.
- [37] M. Sheikholeslami, D. D. Ganji, M. Y. Javed, R. Ellahi, "Effect of thermal

radiation on magneto hydrodynamics nanofluid flow and heat transfer by means of two phase model”, *J. Magn..Mater.* Vol. 374, pp. 36-43, (2015).

[38] M. Turkyilmazoglu, I. Pop, “Heat and mass transfer of unsteady natural convection flow of some nanofluids past a vertical infinite flat plate with radiation effect”, *Int. J. Heat Mass Transfer*, Vol. 59, pp. 167-171, (2013).

[39] M. Sheikholeslami, D. D. Ganjia, M. M. Rashidib, “Ferro fluid flow and heat transfer in a semi annulus enclosure in the presence of magnetic source considering thermal radiation”, *J. Taiwan Inst. Chem. Eng.*, Vol. 47, pp. 6-17, (2015). <http://dxdoi.org/10.1016/j.jtice.2014.09.026>.

[40] D. Pal, “Combined effects of non-uniform heat source/sink and thermal radiation on heat transfer over an unsteady stretching permeable surface”, *Commun. Nonlinear Sci. Numer. Simulat.*, Vol. 16, pp. 1890–1904, (2011).

[41] G. C. Shit, R. Halder, “Effects of thermal radiation on MHD viscous fluid flow and heat transfer over nonlinear shrinking porous sheet”, *Appl. Mathematics Mech. (English Edition)*, Vol. 32, No. 6, pp. 677-688, (2011).

[42] K. Das, “Impact of thermal radiation on MHD slip flow over a flat plate with variable fluid properties”, *Heat Mass Transfer*, Vol. 48, pp. 767-778, (2012).

[43] F. T. Akyildiz, H. Bellout, K. Vajravelu, R.A. Van Gorder, “Existence results for third order nonlinear boundary value problems arising in nano boundary layer fluid flows over stretching surfaces”, *Nonlinear Anal.: Real World Appl.*, Vol. 12, pp. 2919-2930, (2011).

[44] A. J. Chamkha, R. S. R. Gorla, K. Ghodeswar, “Non-similar solution for natural convective boundary layer flow over a sphere embedded in a porous medium saturated with a nanofluid”, *Transp. Porous Media*, Vol. 86, No. 1, pp. 13-22, (2011).

[45] N. Bachok, A. Ishak, I. Pop, “Stagnation-point flow over a stretching/shrinking sheet in a nanofluid”, *Nanoscale Res. Lett.*, Vol. 6, pp. 623-632, (2011).

[46] O. D. Makinde, A. Aziz, “Boundary layer flow of a nanofluid past a stretching sheet with a convective boundary condition”, *Int. J. Thermal Sci.*, Vol. 50, pp. 1326-1332, (2011).

[47] E. M Abo-Eldahab and M. A El-Aziz, “Flow and heat transfer in a micropolar fluid past a stretching surface embedded in a non-Darcian porous medium with uniform free steam”, *Mathematics and Computation*, Vol. 162, No. 2, pp. 881-899, (2005).

**Table 1.** Comparison of the present results with the literature results given by Abo-Eldahab and El-Aziz [47],  $Gc = 0.0, F = 0.0, r = 0.0, Sc = 0.0, Pr = 1.0, Da = 100, \gamma = 0.01, NI = 0.1, G = 2.0, Gr = 2.0, \text{ and } Kr = 0.0$ .

M	$f''(0)$		$g''(0)$	
	Abo-Eldahab and El-Aziz [47 ]	Present	Abo-Eldahab and El-Aziz [47 ]	Present
0.1	0.6708520	0.6708519	- 0.998951	-1.0002098
0.2	0.5717493	0.5717491	- - 0.998905	- 1.0002067

**Table 2.** Variation of  $f''$ ,  $g''$ ,  $-h'$ ,  $\theta'$  and  $\phi'$  at the plate with  $Gr$ ,  $Gc$ ,  $M$ ,  $Da$  and  $\gamma$  for  $N = 0.1$ ,  $G = 2.0$ ,  $Pr = 0.71$ ,  $F = 1.0$ ,  $r = 0.05$ ,  $Sc = 0.6$ ,  $Kr = 0.5$ .

Gr	Gc	M	Da	$\gamma$	$f''(0)$	$g''(0)$	$h'(0)$	$-\theta'(0)$	$-\phi'(0)$
1.0	1.0	0.01	100	0.1	2.03879	-1.0669	0.263381	0.221525	0.698487
2.0	1.0	0.01	100	0.1	3.05663	-1.09305	0.267723	0.190593	0.69596
3.0	1.0	0.01	100	0.1	4.06781	-1.11759	0.271691	0.148666	0.693639
1.0	2.0	0.01	100	0.1	2.7094	-1.08133	0.26557	0.206615	0.697201
1.0	3.0	0.01	100	0.1	3.37401	-1.09525	0.267659	0.18842	0.695971
1.0	1.0	0.03	100	0.1	2.01038	-1.07481	0.26414	0.221955	0.698037
1.0	1.0	0.05	100	0.1	1.98296	-1.08271	0.264898	0.222336	0.697586
1.0	1.0	0.01	10	0.1	1.91849	-1.10242	0.266785	0.223097	0.696464
1.0	1.0	0.01	50	0.1	2.02446	-1.07086	0.26376	0.221746	0.698262
1.0	1.0	0.01	100	0.3	1.82487	-1.14747	0.276459	0.220016	0.690858
1.0	1.0	0.01	100	0.5	1.69724	-1.20516	0.28477	0.218282	0.68592

**Table 3:** Variation of  $f''$ ,  $g''$ ,  $-h'$ ,  $\theta'$  and  $\phi'$  at the plate with  $G$ ,  $Pr$ ,  $N$ ,  $F$ , for  $Gr = 1.0$ ,  $Gc = 1.0$ ,  $M = 0.01$ ,  $Da = 100$ ,  $Sc = 0.6$ ,  $Kr = 0.5$ .

G	Pr	N	F	$f''(0)$	$g''(0)$	$h'(0)$	$-\theta'(0)$	$-\phi'(0)$
2	0.71	0.1	1.0	2.03879	-1.0669	0.263381	0.221525	0.698487
3	0.71	0.1	1.0	2.03789	-1.06794	0.192267	0.221645	0.698542
4	0.71	0.1	1.0	2.03734	-1.06859	0.152723	0.221716	0.698571
2	1.0	0.1	1.0	1.9971	-1.0653	0.263064	0.242647	0.698668
2	2.0	0.1	1.0	1.84742	-1.05963	0.261965	0.345313	0.699296
2	0.71	0.1	2.0	1.99298	-1.06515	0.263036	0.246632	0.698684
2	0.71	0.1	3.0	1.9671	-1.06416	0.262843	0.262791	0.698794
2	0.71	0.1	1.0	2.04179	-1.067	0.263398	0.212343	0.698477
2	0.71	0.1	1.0	2.04634	-1.06715	0.263424	0.198443	0.698462

**Table 4.** Variation of  $f''$ ,  $g''$ ,  $-h'$ ,  $\theta'$  and  $\phi'$  at the plate with  $Sc$  and  $Kr$  for  $Gr = 1.0$ ,  $Gc = 1.0$ ,  $M = 0.01$ ,  $Da = 100$ ,  $G = 2.0$ ,  $Pr = 0.71$ ,  $N = 0.1$ ,  $F = 1.0$ .

Sc	Kr	$f''(0)$	$g''(0)$	$h'(0)$	$-\theta'(0)$	$-\phi'(0)$
0.6	0.5	1.87502	-1.06177	0.262497	0.213985	1.19009
0.78	0.5	1.97791	-1.06484	0.263009	0.223483	0.806176
0.94	0.5	1.93518	-1.06343	0.262759	0.22477	0.893162
0.6	1.0	1.95391	-1.06412	0.262888	0.224133	0.894788
0.6	2.0	1.85936	-1.06118	0.262382	0.226705	1.19012

**How to cite this paper:**

L. Ramamohan Reddy, M. C. Raju, G. S. S. Raju and S. M. Ibrahim, “Chemical reaction and thermal radiation effects on MHD micropolar fluid past a stretching sheet embedded in a non-Darcian porous medium”, *Journal of Computational and Applied Research in Mechanical Engineering*, Vol. 6, No. 2, pp. 27-46

**DOI:** 10.22061/jcarme.2017.582

**URL:** [http://jcarme.srttu.edu/?\\_action=showPDF&article=582](http://jcarme.srttu.edu/?_action=showPDF&article=582)

